

MR Diffusion Tensor Imaging (DTI) and Neuropsychological Testing for Neuronal Connectivity in Alzheimer's Disease (AD) Patients

Jianhui Zhong^{a*}, Hongyan Ni^a, Tong Zhu^a, Sven Ekholm^a, Voyko Kavcic^b
^aDepartment of Radiology, ^bDepartment of Neurology, University of Rochester
601 Elmwood Avenue, Rochester, NY 14642

ABSTRACT

We have used MR DTI to identify relevant brain structures involved in visuospatial processing, in an attempt to link perceptual and attentional impairments to WM changes in Alzheimer's disease (AD) patients. Correlation of DTI measured parameters with results of several neuropsychological tests will be reported here. Several issues related to quantitation of DTI parameters in ROI analysis are addressed. In spite of only a small number of subjects were studied so far, we found not only that AD patients showed significant decrease of white matter (WM) integrity in corpus callosum (CC), most prominent at the posterior portion, but also found significant correlations between the DTI parameters and scores from several neuropsychological tests. Our preliminary results suggest that DTI help to improve the overall accuracy rate in distinguishing between early AD onset and age-related functional decline, and potentially may improve efficiency in differentiating between different types of dementia.

Keywords: MRI, Alzheimer's disease, diffusion tensor imaging, neuronal connectivity, corpus callosum, aging

1. INTRODUCTION

Alzheimer's disease (AD), a neurodegenerative disorder associated with progressive functional decline, is initially diagnosed as a memory disorder accompanied by attentional and perceptual deficits¹⁻³. The perceptual deficits associated with AD include impaired visual motion processing with elevated thresholds for optic flow, the patterned visual motion seen during an observer self-movement⁴⁻⁵. In a recent study we demonstrated that the perceptual impairments observed in AD are linked to temporal constraints on visual attention revealed in rapid serial visual presentations (RSVP)⁶. Based on the RSVP performance of AD patients, we have developed a two-stage concurrent inhibition model of visual perception, the central feature of which is a memory mechanism providing feedback control of input to category specific perceptual processors. This model predicts that an important source of impairment in visual processing is compromised feedback connections from the memory system to the initial perceptual processors. According to our two-stage concurrent inhibition model, we predict sub cortical white matter (WM) alterations at the prefrontal and posterior parietal areas (WM immediately beneath cortex) are related to AD. We also predict that the integrity of WM fibers connecting the prefrontal and posterior parietal cortex (superior longitudinal fasciculus) as well as fibers connecting the two cerebral hemispheres (corpus callosum - CC) may be compromised in AD. In addition, it is hypothesized that the WM fibers of the main afferent/efferent hippocampal tract (cingulum) projecting from and to the cortex are also impaired.

Neurobiologically the hallmarks of AD pathology are amyloid plaques and neurofibrillary tangles which ultimately lead to neuronal loss. Neuronal loss translates to gray matter (synaptic loss) and white matter shrinkage (axonal loss). In the WM, AD neuropathology is associated with decreased volume, most evident in the decrease in size of the corpus callosum (CC)⁷⁻⁹. Previous MR imaging measures (volumetric) describe changes in anatomy only. Recently, it has been demonstrated that diffusion tensor imaging (DTI) can be used as a reliable method for identification of WM tracts and for mapping connectivity between cortical regions¹⁰⁻¹². One of the most widely used DTI measures is fractional anisotropy (*FA*). *FA* is a physical measure of microscopic motion of water at each image location. Reductions in *FA* values in the WM have been identified with degradation of axonal integrity and a loss of cortical connections.

Soon after its advent, DTI was used for investigations of WM changes in AD^{7-9,13}. Rose et al.⁸ showed for the first time that AD patients had significant reduction in anisotropy of WM fiber tracts, such as superior longitudinal

fasciculus, cingulum, and splenium of CC. They also showed significant correlation between lattice index values of splenium and MMSE scores. These findings were replicated by Takashi et al.⁹ who in AD patients found decreased WM *FA* in the posterior part of the CC, temporal lobe, and cingulum. They observed the most robust decrease in WM at the cingulum, particularly at the posterior cingulum. This finding is supported by a more recent report which showed that the earliest changes in AD are found in the posterior cingulate cortex rather than in the hippocampus¹⁴. These initial reports about impaired WM tracts in AD partially correspond to our predictions based on a two-stage concurrent inhibition model, and provide motivation for us to pursue a DTI study, aiming at quantitative analysis of DTI parameters and correlation to several neuropsychological tests in AD patients.

Here we present our initial findings obtained with DTI in AD patients and age-matched controls for the CC alone and how the integrity of WM correlates with performance on some neuropsychological tests. There are two main reasons that we initially investigated integrity of WM in the CC: firstly, CC is the most prominent WM structure in the brain and also the easiest to identify and measure in MRI. Secondly, CC is implicated to be a region of interest (ROI) not only from the perspective of our model, but also because some researchers have conceptualized AD as a disconnection syndrome. The neuroanatomical loss of connectivity in AD has been supported by imaging studies that reported a significant loss in CC volume¹⁵⁻¹⁸. Longitudinal studies found that AD patients showed significantly greater rates of CC atrophy than age-matched controls^{16,19-20}. Above cited studies reported an overall decline in WM associated with advanced age, but the rate of decline was greater in AD patients. In addition, there is some behavioral evidence that AD patients are impaired in tasks which require cross-callosal communication²¹.

2. NEUROPSYCHOLOGICAL TESTS AND IMAGING PROTOCOL

2.1 Subject Groups

We studied 5 Alzheimer's Disease (AD) patients without ophthalmological or other neurological disorders (age 70-85, mean 75.8), and 11 age-matched normal (ON) control subjects (age 63-91, mean 77.9). All had normal, or corrected to normal, visual acuity and contrast sensitivity. Five AD subjects were recruited from the clinical programs of the University of Rochester Alzheimer's Disease Center with probable AD by NINDS criteria²². The ON subjects were recruited from programs for the healthy elderly or were the spouses of AD subjects (see Table 1 for detailed information). Informed consent was obtained from all subjects before their participation. All procedures were approved by the University of Rochester Human Subject Review Board and complied with the Declaration of Helsinki.

2.2 Neuropsychological evaluation

Neuropsychological tests for evaluation of basic cognitive capacities included:

- (1) Mini-Mental Status Examination (MMSE)²³ was used as a measure of overall impairment in dementia. The test is comprised of a restricted set of short cognitive tests that includes: a test for time and location orientation, registration, naming, figure copying, attention and recall. Maximal score is 30. Normal performance scores range from 27 – 30; mild impairment scores range from 20 - 27.
- (2) The Road Map test²⁴ was used to assess topographic orientation on a simulated route. The test consists of a map of a city. The subject must follow the route at the experimenter's prompts to turn left or right at each intersection. The performance is expressed in terms of correct turns, with a maximum score of 32.
- (3) Verbal Paired Associates test from the Wechsler Memory scale²⁵ was used to assess immediate and delayed verbal memory. The test contains 8 word pairs half of which form "easy" associations (e.g., baby - cries) and the other half form "hard" associations (e.g., cabbage - pen). The list of word pairs is read at least 3 times or as many as needed for an errorless score (up to 6 readings). Following each reading there is a memory test (i.e., recall). The subject has to recall the word from the missing word pair after being presented with the other word. Maximum score is 24.
- (4) Delayed Memory test from the Wechsler Memory scale²⁵ was used to assess delayed verbal memory. After 20 minutes delay, the subject is once again tested for recall on word pairs. Maximum score is 8.
- (5) Figural Memory test from the Wechsler Memory scale²⁵ was used to assess immediate visual recognition. The test is made up of 4 trials, each with one to three abstract rectangular designs. After the subject has been shown the target designs for 5 seconds per design, the design is removed and the subject must identify them from an array of similar designs. Maximum score is 10.

- (6) The Category Name Retrieval test was used to assess memory retrieval and cognitive flexibility. In this test the subject must name as many animals as possible within 60 seconds. The test is open-ended, with a score below 12 indicative of memory impairment.
- (7) The Judgment of Line Orientation test²⁶ was used to test the ability to judge angular relationships between line segments by visually matching angled line pairs with 11 numbered lines arranged in a semicircle. The test consists of 30 items, each showing a different pair of angled lines to be matched to the sample.
- (8) The Facial Recognition²⁶ test was used to assess visuospatial processing without involving mnemonic processes. The subject matches identical faces from the front view with faces presented in side views, three-quarter views, and front views taken under different lighting conditions. There are 52 matches in total.

Total time for all neuropsychological tests was under 60 min.

2.3 MR imaging protocol

All MR examinations were performed on a GE Signa 1.5 T MR scanner with echo-speed gradients and LX9.1 software. A quadrature head coil was used for all acquisition. All subjects were scanned with the following pulse sequences:

- (1) A three-orientation scout imaging T1W sequence for localization;
- (2) 3D Coronal fast SPGR sequence for whole brain anatomy and co-registration with DTI, with variable bandwidth and enhanced dynamic range, TR/TE/FA=19/min/25, 256x256 matrix size, slice thickness=1.2mm, FOV=24cm, loc/slab=128;
- (3) Whole brain isotropic DTI imaging in coronal orientation, with a single-shot pulsed-gradient spin-echo echo-planar sequence and the following parameters: TR/TE = 4000/116 ms, matrix size = 128x128, FOV = 24 cm, thickness=3.5mm, with 2 repetitions in each diffusion orientation. Diffusion weighting was applied in 20 different orientations with gradient b value = 0 and 1000 s/mm². Images cover anatomic structures including the sub cortical WM in the bilateral, frontal and posteroparietal areas, bilateral fronto-posteroparietal superior bundles, bilateral anterior and posterior cingulum, and the anterior (genu) and posterior (splenium) portion of CC.
- (4) Brain coronal DTI imaging, with similar pulse sequence as in (3), but only cover selected brain regions (anterior, middle, and posterior CC). Diffusion weighting was applied in 30 different orientations with gradient b value = 0 and 1000 s/mm²;
- (5) Coronal FLAIR images of the same locations as in (2), resulting in high resolution T2W images with well defined GM/WM differentiation and fine structures.

Total scanning time was under 45 min.

3. IMAGE AND STATISTICAL ANALYSES

3.1 Image measurements

Images from DTI acquisition were processed on PCs for tensor calculations, including diffusion eigenvalues and eigenvectors, from which fractional anisotropy (FA) maps were created. Color WM track directional map based on FA values were also generated. These steps of processing were performed by using the VOLUME-ONE software provided by the VOLUME-ONE developer group and available on the Internet (<http://www.volume-one.org>).

The output from the above processing was further analyzed. As a first step in the quantitative analysis of these images, regions of interest (ROIs) analysis was performed and results are reported in this article. ROIs consisting of certain numbers of pixels were placed in the selected regions (such as corpus callosum (CC), cingulum, and cortical WM), statistical distributions of relevant DTI parameters were collected, and the results were tabulated for all subjects for further analysis. The processing codes are written in Matlab (Mathworks, Natick, MA). More details of these analyses are given below.

Definitions of DTI parameters

For each diffusion-weighted image, signal intensity can be related to apparent diffusion coefficient (ADC) along a particular spatial orientation by

$$S_{ij} = S_0 \exp(-b_{ij} ADC_{ij}),$$

where S_0 and S_{ij} represent the image intensity with no gradients ($b=0$) or with gradient applied along the orientation of b_{ij} , and b is the gradient factor. For all the measurements in this study, $b = 1000 \text{ s/mm}^2$ was used.

For all diffusion-weighted images, the general diffusion tensor was first diagonalized, and the yielded scalars invariants of the tensor, including the eigenvalues λ_1 , λ_2 , and λ_3 were derived for every image pixel. As index of degree of anisotropy, we used fractional anisotropy (FA , dimensionless, ranging from 0.0 for perfectly isotropic diffusion, to 1.0 for perfectly anisotropic diffusion), which is defined as

$$FA = \sqrt{\frac{2}{3} \frac{\sqrt{(\lambda_1 - \langle D \rangle)^2 + (\lambda_2 - \langle D \rangle)^2 + (\lambda_3 - \langle D \rangle)^2}}{\sqrt{\lambda_1^2 + \lambda_2^2 + \lambda_3^2}}},$$

where $\langle D \rangle$ is the average of the trace of the diffusion tensor \mathbf{D} :

$$\langle D \rangle = \frac{1}{3} \text{Tr}(\mathbf{D}) = \frac{1}{3} (\lambda_1^2 + \lambda_2^2 + \lambda_3^2).$$

ROI analysis

We have developed a series of Matlab codes with graphic user interfaces (GUIs), which loads a complete set of image data, and interpolates so that isotropic 3D images of DWI, and ADC and FA maps can be displayed in all 3 orientations (AP/LR/SI). GUIs are provided so that a user can select ROIs of pre-defined (rectangular or circular) or arbitrary shapes and sizes. Histograms of relevant DTI parameters (ADC , FA , eigenvalues) are then calculated in the accumulated ROIs (single or multiple regions).

Since CC is surrounded by cerebrospinal fluid (CSF), which is essentially “pure water” and has very high ADC and very low FA values, contamination of CSF into WM ROIs can severely skew the results of ADC and FA calculations. Therefore, three levels of handling of ROI data are built into the processing codes to evaluate the CSF effects: without any filter; with a low-pass filter to eliminate contributions of CSF pixels to ADC values in the selected ROIs based on the measured ADC value for CSF; and a low-pass filter of ADC based on a fixed value, to eliminate possible contaminations due to partial volume effects in pixels with mixture of CSF/tissue. Distributions of ADC and FA values of the remaining pixels are then calculated. A threshold value of $ADC = 1.7$ is empirically determined. Effects of these filters are demonstrated in Fig. 1. It can be seen that along three levels of filtering, mean ADC values decrease, and mean FA values increase, while the mean values come closer to the median values of ADC or FA , which indicate that they are approaching a normal distribution. Moreover, acquisitions with both thin (3.5 mm) and thick (7 mm) slices for images introduce minimum partial volume effect.

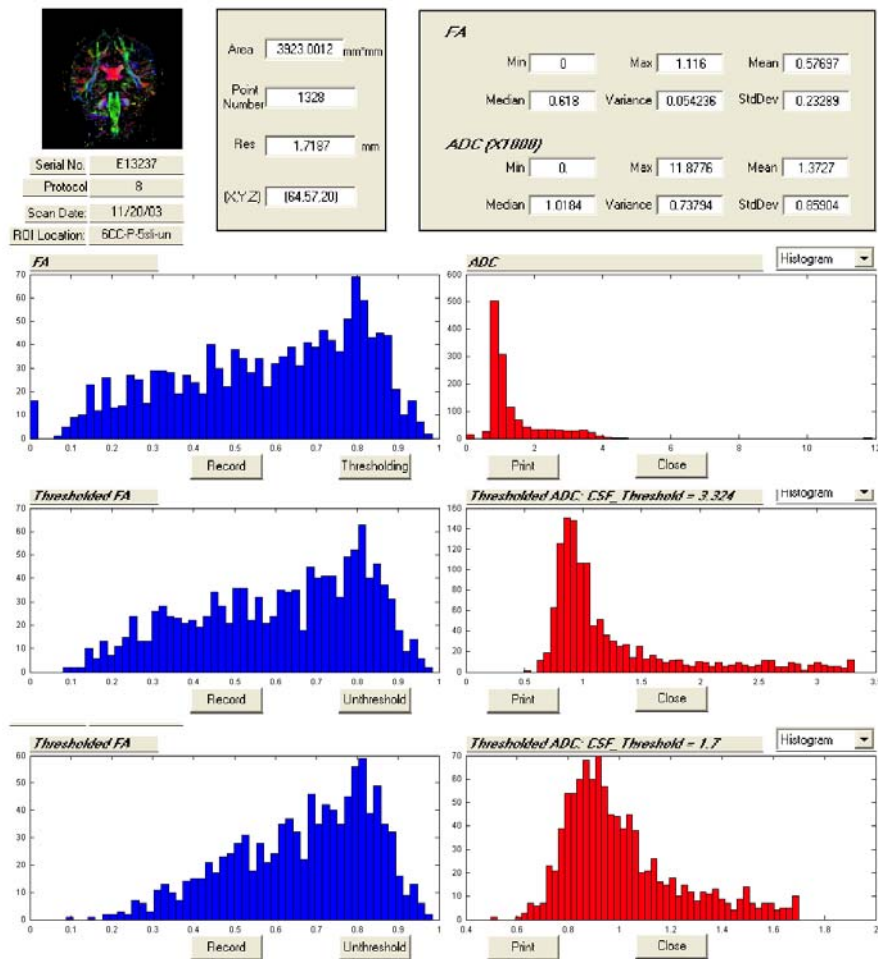


Fig. 1. GUI for statistical calculations in selected ROIs, with CC selected in the posterior section. Histograms below the GUI are for *FA* and *ADC* from measurements without any filter (top), with pixels of *ADC* values equal to or less than what is measured for CSF (middle), and with pixels of *ADC* values less than a fixed threshold (=1.7). The table below summarizes results from these histograms with two acquisition protocols.

For each parameter, the one in the first row below is mean±std, and the one in the second row is median±variance.

Slice thick = 3.5mm:

Filter	ADC	FA
No	1.37±0.86	0.577±0.232
	1.02±0.74	0.618±0.054
CSF	1.26±0.62	0.605±0.210
	1.00±0.39	0.639±0.044
Fixed	1.01±0.22	0.665±0.172
	0.95±0.52	0.696±0.030

Slice thickness=7mm:

Filter	ADC	FA
No	1.46±0.89	0.580±0.218
	1.06±0.80	0.603±0.048
CSF	1.32±0.66	0.597±0.206
	1.04±0.44	0.619±0.042
Fixed	1.03±0.24	0.654±0.176
	0.97±0.05	0.677±0.031

3.2 Statistical correlation of DTI and neuropsychological tests

Due to the small sample size and potential violation of assumption of normality, nonparametric tests were used: the Mann-Whitney test for evaluation of differences between AD and ON group, and the Spearman's rank correlation coefficient for evaluation of association between DTI measures and performance scores on neuropsychological tests.

4. RESULTS

In this article, only results from ROI analysis in the CC will be reported. Examples of *FA* color maps and definitions of ROIs in anterior, middle, and posterior portions of CC are shown in Fig. 2.

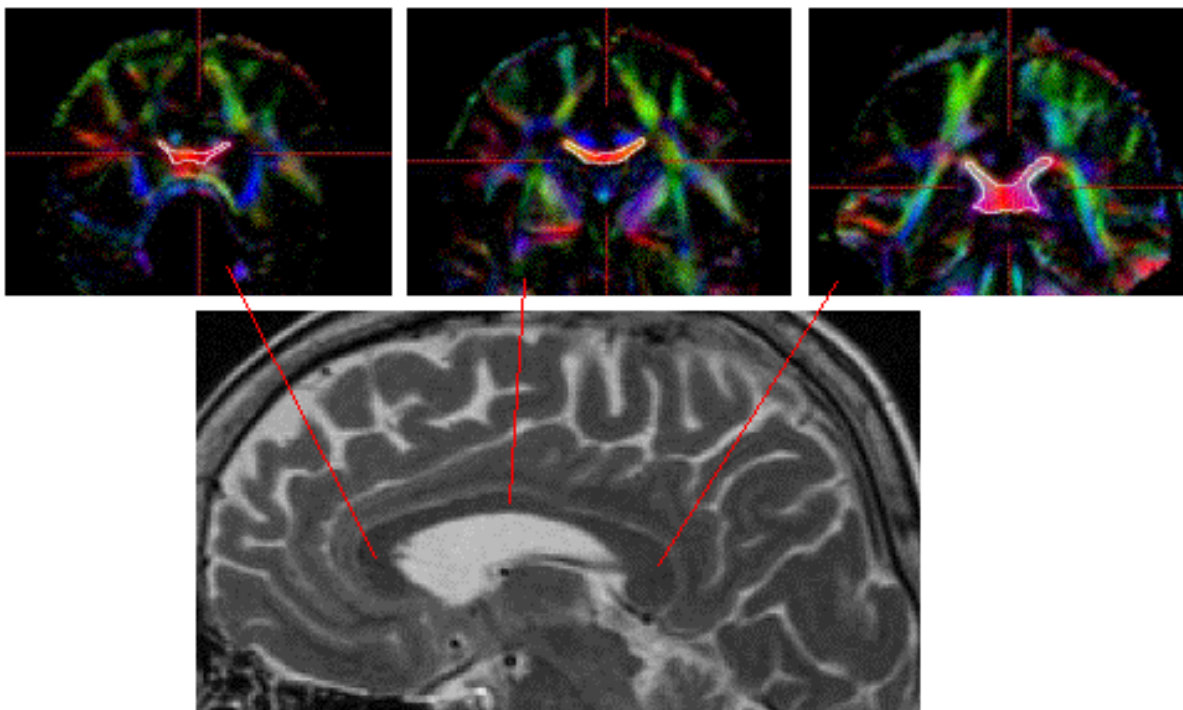


Fig. 2. T2-weighted sagittal anatomical image (below), and colored directional *FA* maps (top) for a control subject, covering the anterior (left), middle (middle) and posterior (right) portion of corpus callosum. These areas are outlined white lines. ROI measurements are from pixels similarly defined in 4–5 adjacent slices in each portion of CC.

4.1 DTI measurements

Despite a small sample size in the study, the results indicate that there is a statistically significant difference between AD patients and age-matched controls. The mean *FA* values for the three regions of the CC, obtained with 5 AD patients and 11 age-matched controls, are presented in Fig 3 (a), and the mean *ADC* values are presented in Fig 3 (b). On both measures, AD patients showed significantly different values than age-matched controls: marginally smaller *FA* values at the anterior ($p = .07$) and significantly smaller *FA* at the posterior CC ($p = .004$); greater *ADC* values at the posterior CC ($p = .02$). Note also that the DTI measures differed significantly between the three sites for both groups: the highest average *FA* value was obtained from the middle section of the CC, followed by anterior section of CC, and the lowest *FA* value from the posterior section of CC. The trend was the reverse for *ADC*: the highest average *ADC* was obtained at the posterior section of CC, followed by anterior section, and the lowest from the middle section of CC.

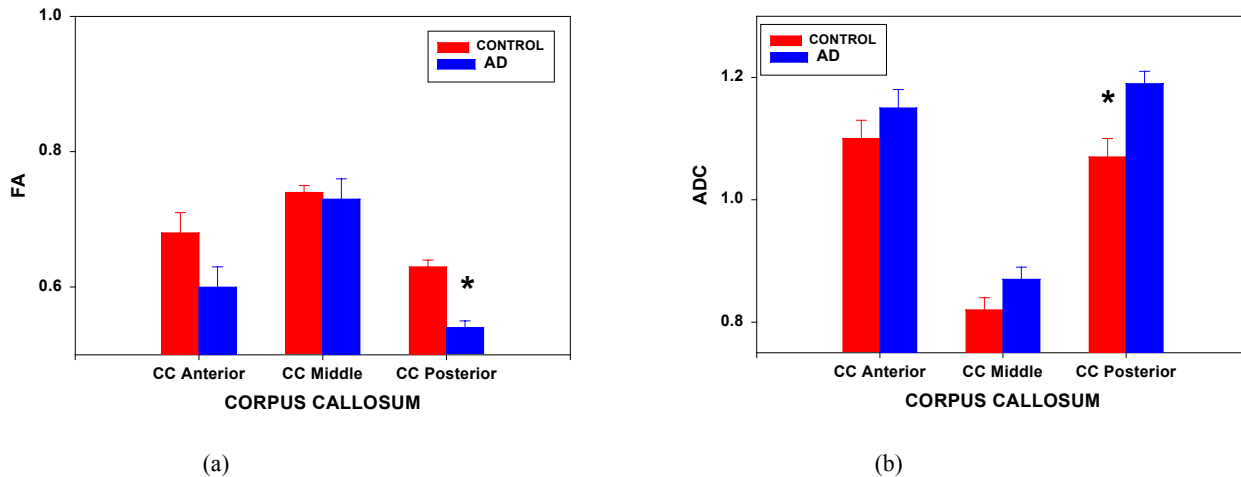


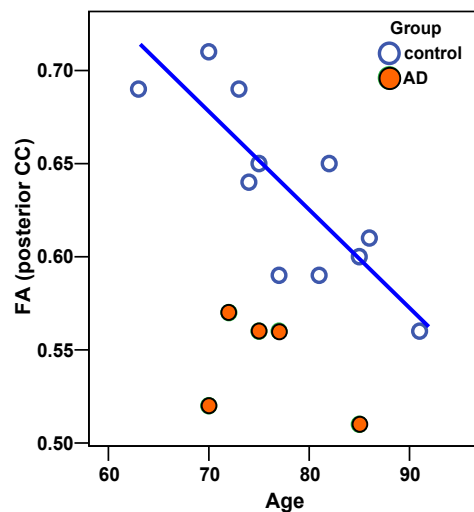
Fig 3 (a). Mean FA values at anterior, middle, and posterior sites of the corpus callosum (CC); (b) Mean ADC values at anterior, middle, and posterior sites of the corpus callosum (CC). Asterisk * indicates a statistically significant difference ($p < 0.05$) among the two groups.

4.2 Association between DTI measures and performance on neuropsychological test

TEST	GROUP	
	AD	Controls
Age	75.8	77.9
MMSE	22.4	28.8**
Money Road Map	24.6	31.3**
Figural Memory	4.4	7**
Verbal Paired Associates	8	17.1**
Delayed Recall	3	6.9*
Verbal Fluency	11	22.5**
Line Orientation	13.4	25.8**
Facial Recognition	42.4	47.8

The mean age and mean scores on 8 neuropsychological tests are presented in the Table on the left.

AD patients do not differ from ON in age, but their performance is significantly lower in all neuropsychological tests, except the Facial Recognition test. Thus, the performance profile on the neuropsychological test additionally confirms that our AD patients fit the profile of cognitive impairments due to Alzheimer's disease.



Results did not reveal any significant correlations between DTI measures and performance score for ON. However, ON showed a high correlation between age and FA values only from the posterior CC ($r = .78$, $p = .005$), whereas AD did not show any correlation (Fig 4).

Fig. 4. Scatter plot diagram illustrating the relationship between FA values in the posterior CC and age in controls.

For AD patients, on the other hand, there were statistically significant correlations between FA and

ADC values and performance on several neuropsychological tests indicating that a better performance on the test was correlated with higher integrity of white matter. The AD group showed a significant correlation between FA from the anterior CC and Figural Memory ($r = .89, p = .04$) (Fig. 5 a) and between FA from the middle CC and the Judgement of Line Orientation test ($r = .99, p = .001$) (Fig. 5 b). ADC from the middle CC significantly correlated with the score on the Face Recognition test ($r = -.87, p = .05$).

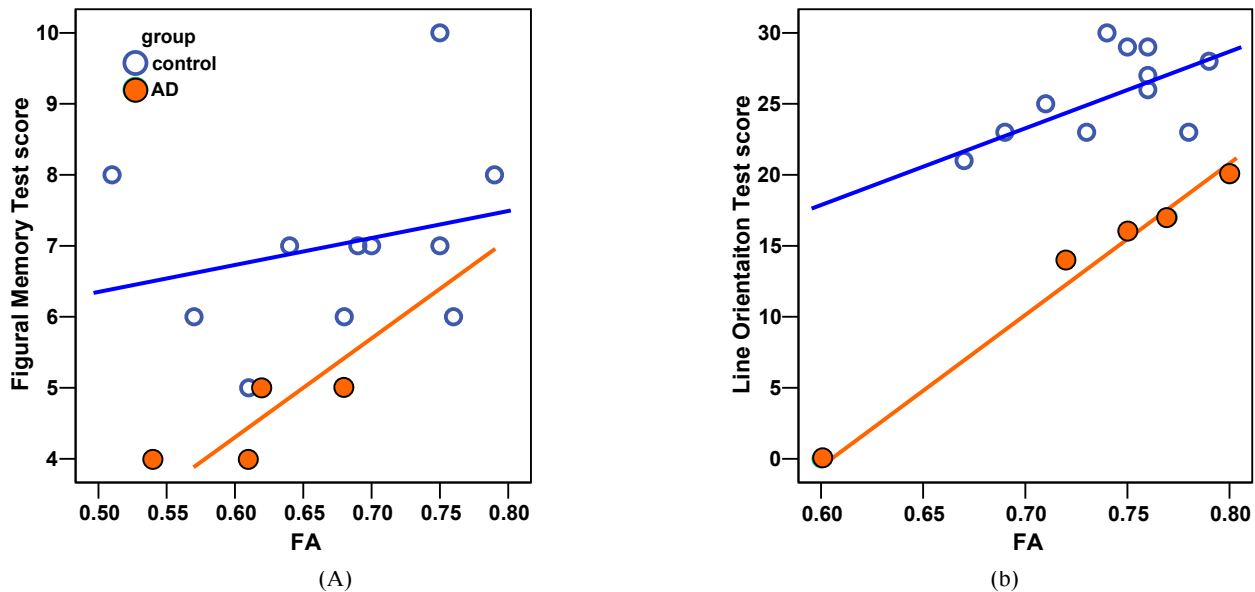


Fig. 5. Scatter plot diagram illustrating the relationship between *FA* values from anterior CC and scores on Figural Memory test (a), and between *FA* values from middle CC and scores on Line Orientation test (b).

5. DISCUSSION AND CONCLUSIONS

The main observations of this study are: (1) WM integrity of the posterior CC, as measured by *FA* and *ADC*, significantly decrease with age in ON; (2) Early stage AD patients have decreased integrity of WM in the CC, beyond what is related to normal aging. It is most evident in the splenium and to the lesser degree in the genu, but not in the body of CC; (3) Decreased integrity of WM in AD is associated with decreased performance in some neuropsychological test, particularly in those measuring visuospatial capacities. Before discussing these results in more detail, it is pertinent to address some methodological and technical aspects of this study.

Technical aspects

We have shown that with low-pass *ADC* filters of different level, contaminations of CSF pixels or partial CSF/tissue pixels can be effectively minimized for ROI analyses. The effectiveness of the method was demonstrated by approaching the normal distributions with more filtering, and a minimal difference between results from thin-slice and thick-slice images. This step is important because CSF has much higher *ADC* and much lower *FA* values, and it would severely skew the distribution of these values in tissues even when only a few pixels were included in the ROI for calculation. Results of these analyses allow us to separate true pathological *ADC* increase/*FA* decrease related to AD from possible contaminations of CSF, and obtain tight correlations between the DTI and neuropsychological measurements with a small number of subjects. To further address issues of atrophy and vascular mild cognitive impairment (MCI), we will use acquired FLAIR and 3D SPGR images to segment brain tissue types, and use the segmented images for analyzing changes in DTI parameters in different regions.

There have been studies showing that the principal eigenvalues of diffusion tensor may provide additional information about neuron degeneration²⁷ in complement to the *FA* values. Co-registration of DTI with other images and selection of ROIs based on the segmented high-resolution images may prove to be more accurate. The relevance and usefulness of the methods for image co-registration and transformation to the standard coordination system (such as Talairach) are also under evaluation²⁸. Evaluations of these issues are in progress in our research labs.

Aging aspects

Several researchers^{29-30,19,31-32} reported decreased integrity of WM with advanced age. O'Sullivan et al.¹⁹ found decreased *FA* in the prefrontal region. Other groups^{29,31-32} reported decreased *FA* values only in the anterior portion of CC while Nusbaum et al.³⁰ found *FA* reduction in both the anterior and posterior portions of the CC. Our findings partially agree with those of Nusbaum et al.³⁰. There are several possible sources of discrepancies between the studies, ranging from the definition of the ROIs, to scanning procedure, and subject age range. It may also relate to details in quantitation (such as issues discussed above). The tentative explanation for the decline in WM integrity with advanced age may reflect mild structural changes associated with normal aging³⁶. Postmortem histological analyses have also indicated a loss of myelinated fibers in normal aging. Decreased integrity of WM in splenium may be related either to anatomical features of the splenium (i.e., greater number of larger diameter myelinated fibers in the splenium than in the body of CC; ref 33) or to the aging process (i.e., greater decrease in *FA* in the splenium than in other parts of CC; ref 34).

Clinical aspect of AD

Similar to this study, significant reductions in *FA* values in the posterior CC in AD patients have been previously observed by other researchers^{9,35}. Reductions in the *FA* values suggest either a reduction in number of axons, degeneration of myelin tissue, or changes in axonal processes. It has been demonstrated that AD causes partial myelin loss, and loss of axons and oligodendroglial cells accompanied by a mild reactive astrogliosis³⁷. These WM changes occur independently of gray matter processes. The decrease in *FA* values and the corresponding increase in ADC in AD could reflect a primary disintegration of myelin and impairments in axonal flow or being a secondary effect due to neuronal death and subsequent axonal degeneration. The decrease in *FA* in the posterior portion of the CC most likely reflects the spread of AD neuropathology. This progresses from the medial temporal structures (e.g., from entorhinal cortex to hippocampus) to the temporal cortex, followed by the posterior parietal areas and, to a varying degree the prefrontal cortex³⁸⁻³⁹.

To our knowledge, this is the first report demonstrating that disintegration of WM suggested by the reduced *FA* values in CC in mildly impaired AD patients is significantly correlated with a degraded performance on standard neuropsychological tests. This association was most remarkable for tests measuring visuospatial capacity and changes in the anterior and middle portion of CC. However, these correlations between integrity of WM in CC and performance on some neuropsychological test must be taken cautiously because of the small sample of AD patients. Several researchers have shown that the majority of AD patients exhibit impaired performance in tests for visuospatial capacities (for a summary, see ref 2). It has been hypothesized that such impairment reflects the spread of AD neuropathology to the posterior parietal cortex, an area crucial for visuospatial processing. We present additional evidence indicating that in the earlier stages of AD neuropathology there is not only an affect on functioning (i.e., visuospatial processing) but also on structure (WM). Focal disruption of commissural connectivity, as evidenced by decreased *FA* and increased ADC, may cause this decrease in performance on visuospatial tests.

CC is not the only region in the brain where disintegration of WM can be detected in AD. Others⁷⁻⁹ have shown disintegration of WM in regions such as superior longitudinal fasciculus, cingulum, hippocampus, and temporal lobe. Further research is needed to clarify relations between all these regions and how are all these regions implicated in cognitive networks.

Our main objective for the long-term study is to link perceptual and attentional impairments to WM changes by identifying relevant brain structures involved in visuospatial processing. Our objective is also to validate DTI as a new diagnostic tool for early AD. Many more technical developments are needed towards these objectives. High spatial resolution tractography of DTI may be needed to establish neuroconnectivity and feedback circuitry to evaluated models

such as the RSVP. It can be anticipated however that in the near future DTI will not only help to improve the overall accuracy in distinguishing between early AD onset and age-related functional decline, but will also improve efficiency in differentiating between different types of dementia; additionally, it will assist in differentiating dementias from other neurological and psychiatric disorders. It should also allow us to track the progression of AD by means of evaluating microstructural regional changes and atrophy in WM. In addition, DTI measures may become sensitive enough to detect the effects of pharmacological interventions on the microstructure of WM.

ACKNOWLEDGEMENT

This work was partially supported by the NIH under Grants NS32024 and NS41048, and an internal pilot research pilot grant from the Center for Visual Science, University of Rochester.

REFERENCES

1. Cummings, J. L. (2000). Cognitive and behavioral heterogeneity in Alzheimer's Disease: Seeking the neurobiological basis. The Neurobiology of Aging, *21*, 863-864.
2. Parasuraman, R. & Greenwood, P. M. (1998). Selective Attention in Aging and Dementia. In R.Parasuraman (Ed.), The Attentive Brain (pp. 461-487). Cambridge, USA: MIT Press.
3. Mesulam, M. (2000). Principles of behavioral and cognitive neurology. New York, NY, Oxford University Press, Inc.
4. O'Brien, H. L., Tetewsky, S., Avery, L. M., Cushman, L. A., Makous, W., & Duffy, C. J. (2001). Visual mechanisms of spatial disorientation in Alzheimer's disease. Cerebral Cortex, *11*, 1083-1092.
5. Tetewsky, S. & Duffy, C. J. (1999). Visual Loss and Getting Lost in Alzheimer's Disease. Neurology, *52*, 958-965.
6. Kavcic, V. & Duffy, C. J. (2003). Attentional dynamics and visual perception: mechanisms of spatial disorientation in Alzheimer's disease. Brain, *126*, 1173-1181.
7. Bozzali, M., Franceschi, M., Falini, A., Pontesilli, S., Cercignani, M., Magnani, G., Scotti, G., Comi, G., & Filippi, M. (2001). Quantification of tissue damage in AD using diffusion tensor and magnetization transfer MRI. Neurology, *57*, 1135-1137.
8. Rose, S. E., Chen, F., Chalk, J. B., Zelaya, F. O., Strugnell, W. E., Benson, M., Semple, J., & Doddrell, D. M. (2000). Loss of connectivity in Alzheimer's disease: an evaluation of white matter tract integrity with colour coded MR diffusion tensor imaging. Journal of Neurology, Neurosurgery & Psychiatry, *69*, 528-530.
9. Takahashi, S., Yonezawa H., Takahashi J., Kudo, M., Inoue T., & Tohgi, H. (2002). Selective reduction of diffusion anisotropy in white matter of Alzheimer disease brains measured by 3.0 Tesla magnetic resonance imaging. Neuroscience letters, *332*, 45-48.
10. Basser PJ, Mattiello J, LeBihan D (1994). MR diffusion tensor spectroscopy and imaging. Biophysical Journal *66*(1):259-267.
11. Pierpaoli C, Barnett A, Pajevic S, Chen R, Penix LR, Virta A, Basser P (2001). Water diffusion changes in Wallerian degeneration and their dependence on white matter architecture. Neuroimage *13*(6 Pt 1):1174-1185.
12. Basser PJ, Pajevic S, Pierpaoli C, Duda J, Aldroubi A (2000). In vivo fiber tractography using DT-MRI data. Magn Reson Med *44*(4):625-632.
13. Bozzao A, Floris R, Baviera ME, Apruzzese A, Simonetti G (2001). Diffusion and perfusion MR imaging in cases of Alzheimer's disease: correlations with cortical atrophy and lesion load. AJNR Am J Neuroradiol *22*(6):1030-1036.
14. Minoshima, S., Giordani, B., Berent, S, Frey, K. A, Foster, N. L., & Kuhl, D. E. (1997). Metabolic reduction in the posterior cingulate cortex in very early Alzheimer's disease. Annals of Neurology, *42*, 85-94.
15. Black, S. E., Moffat, S. D., Yu, D. C., Parker, J., Stanchev, P., & Bronskill, M. (2000). Callosal atrophy correlates with temporal lobe volume and mental status in Alzheimer's disease. Canadian Journal of Neurological Sciences, *27*, 204-209.

16. Hampel, H., Teipel, S. J., Alexander, G. E., Pogarell, O., Rapoport, S. I., & Moller, H. J. (2002). In vivo imaging of region and cell type specific neocortical neurodegeneration in Alzheimer's disease - Perspectives of MRI derived corpus callosum measurement for mapping disease progression and effects of therapy. Evidence from studies with MRI, EEG and PET. Journal of Neural Transmission, *109*, 837-855.
17. Hensel, A., Wolf, H., Kruggel, F., Riedel-Heller, S. G., Nikolaus, C., Arendt, T., & Gertz, H. J. (2002). Morphometry of the corpus callosum in patients with questionable and mild dementia. Journal of Neurology Neurosurgery and Psychiatry, *73*, 59-61.
18. Teipel, S. J., Hampel, H., Pietrini, P., Alexander, G. E., Horwitz, B., Daley, E., Moller, H. J., SCHAPIRO, M. B., & Rapoport, S. I. (1999). Region-specific corpus callosum atrophy correlates with the regional pattern of cortical glucose metabolism in Alzheimer disease. Archives of Neurology, *56*, 467-473.
19. O'Sullivan, M., Summers, P. E., Jones, D. K., Jarosz, J. M., Williams, S. C., & Markus, H. S. (2001). Normal-appearing white matter in ischemic leukoaraiosis: a diffusion tensor MRI study. Neurology, *57*, 2307-2310.
20. Teipel, S. J., Bayer, W., Alexander, G. E., Zebuhr, Y., Teichberg, D., Kulic, L., Schapiro, M. B., Moller, H. J., Rapoport, S. I., & Hampel, H. (2002). Progression of corpus callosum atrophy in Alzheimer disease. Archives of Neurology, *59*, 243-248.
21. Lakmache, Y., Lassonde, M., Gauthier, S., Frigon, J. Y., & Lepore, F. (1998). Interhemispheric disconnection syndrome in Alzheimer's disease. Proceedings of the National Academy of Sciences of the United States of America, *95*, 9042-9046.
22. McKhann G, Drachman D, Folstein M, Katzman R, Price D, Stadlan EM. Clinical diagnosis of Alzheimer's disease: report of the NINCDS-ADRDA Work Group under the auspices of Department of Health and Human Services Task Force on Alzheimer's Disease. Neurology 1984; 34: 939-944.
23. Folstein, M. F., Folstein, S. E., & McHugh, P. R. (1975). "Mini-mental state". A practical method for grading the cognitive state of patients for the clinician. Journal of Psychiatric Research, *12*, 189-198.
24. Money, J. (1976). A Standardized Road Map Test of Direction Sense. San Rafael, CA., Academic Therapy Publications.
25. Wechsler, D. (1987). Wechsler Memory Scale Manual. San Antonio, TX; The Psychological Corporation.
26. Benton, A.L., Hamsher, K deS., Varney, N.R., & Spreen, O. (1983). Contributions to neuropsychological assessment. New York; Oxford University Press.
27. Glenn OA, Henry RG, Berman JI, Chang PC, Miller SP, Vigneron DB, Barkovich AJ (2003). DTI-based three-dimensional tractography detects differences in the pyramidal tracts of infants and children with congenital hemiparesis. J Magn Reson Imaging 18(6):641-648
28. Xu D, Mori S, Shen D, van Zijl PC, Davatzikos C (2003). Spatial normalization of diffusion tensor fields. Magn Reson Med 50(1):175-182.
29. Abe, O., Aoki, S., Hayahashi, N., Yamada, H., Kunimatsu, A., Mori, H., Yoshikawa, T., & Ohtomo K. (2002). Normal aging in the central nervous system: quantitative MR diffusion-tensor analysis. Neurobiology of Aging, *23*, 433-441.
30. Nusbaum, A.O., Tang, C.Y., Buchsbaum, M.S., Wei, T.C., & Atlas, S.W. (2001). Regional and global changes in cerebral diffusion with normal aging. American Journal of Neuroradiology, *22*, 136-142.
31. Pfefferbaum, A., Sullivan, E.V., Hedelus, M., Lim, K.O., Adalsteinsson, E., & Moseley, M. (2000). Age-related decline in brain white matter anisotropy measured with spatially corrected echo-planar diffusion tensor imaging. Magnetic Resonance Medicine, *44*, 259-268.
32. Sullivan, E.V., E.V., Adalsteinsson, E., Hedelus, M., Ju, V., Moseley, M., Lim, K.O., & Pfefferbaum, A. (2001). Equivalent disruption of regional white matter microstructure in ageing healthy men and women. Neuroreport, *12*, 99-104.
33. Aboitiz, F., Rodriguez, E., Olivare, R., & Zaidel, E. (1996). Age-related changes in fibre composition of the human corpus callosum: sex difference. Neuroreport, *7*, 1761-1764.
34. Aboitiz, F., Scheibel, A.B., Fisher, R.S., & Zaidel, E. (1991). Fiber composition of the human corpus callosum. Brain Research, *598*, 143-153.
35. Hanyu, H., Asano, T., Sakurai, H., Imono, Y., Iwamoto, T., Takasaki, M., Shindo, H., & Abe, K. (1999). Diffusion-weighted and magnetization transfer imaging of the corpus callosum in Alzheimer's disease. Journal of Neurological Science, *167*, 37-44.
36. Tang, Y., Nyengaard, J.R., Pakkenberg, B & Gundersen, H.J. (1997). Age-induced white matter changes in the human brain: a stereological investigation. Neurobiology of Aging, *18*, 609-615.

37. Brun, A. & Englund, E. (1986). A white matter disorder in dementia of the Alzheimer type: a pathoanatomical study. Annals of Neurology, 19, 253-262.
38. Braak, H. & Braak, E. (1995). Staging of Alzheimer's disease-related neurofibrillary changes. [Review] [45 refs]. Neurobiology of Aging, 16, 271-278.
39. Van Hoesen, G. W. (2002). The human parahippocampal region in Alzheimer's Disease, dementia, and aging. In M.P.Witter & F. Wouterlood (Eds.), The parahippocampal region: Organization and role in cognitive function (pp. 271-295). Oxford: Oxford University Press.